

S.P. MOGHADAM AND J.C. RADON*

This paper discusses the fatigue crack propagation in the base material and the weldment of structural steel BS 4360-50D used in offshore structures. The base material and the weldments were tested at R -values of 0.08 and 0.7 at a loading frequency of 0.25 Hz. To investigate the effect of frequency on crack growth rate some other tests were performed on both base metal and the weldment at a cyclic frequency of 30 Hz. All the specimens were tested in the 'as-received' condition, and tests were performed in laboratory air at 20°C. The stress ratio and frequency of loading were found to have a significant effect on the fatigue crack propagation behaviour of the base metal. Fatigue crack growth rates in the weldments were similar to or slower than in the base material, probably due to favourable residual stresses. The fractography of the weldments was performed using a standard SEM. The influence of defects in the weld beads was investigated. The deleterious effect of secondary cracking, damage and porosity on the crack growth rate was also noted.

INTRODUCTION

Failure of engineering structures subjected to repeated load is usually caused by the initiation of subcritical cracks and their subsequent growth to a critical size at which fast fracture occurs. Depending on the structure and its design, the initiation and propagation phases may occupy a smaller or larger part of the useful service life. In large installations, such as offshore platforms, and particularly in welded structures, small crack-like defects are invariably present from the time of their commissioning.

Although a large amount of work has been completed on characterising the fatigue crack growth properties of structural materials such as the steel used in the present investigation, there are conflicting reports as to how certain mechanical and metallurgical factors affect the fatigue crack growth rate. Also, relatively little work has been done on characterising the fatigue crack growth properties of weldments developed specially for these oil platforms. Fatigue crack propagation in BS4360 was investigated by Musuva(1) using the LEFM approach. However, for fatigue cracks in a weldment, the applicability of fracture mechanics is not so straightforward because of the internal defects often observed in an otherwise sound weld. Fatigue cracks may initiate from these internal defects or from regions of high stress concentration, due to the sharp microscopic slag inclusions that are found to be an inherent feature of welds, particularly when produced by manual arc welding methods (2). In order to apply fracture mechanics to weldments, the applicability of some cyclic crack propagation law has to be investigated. The factors which control the stress state at the crack tip may substantially affect the crack growth rate. These include the fracture mode, plastic zone size, microstructure and environment. The objective of the present work was to compare the fatigue crack growth properties of the base metal and the weldment in identical mechanical and environmental conditions.

* Department of Mechanical Engineering, Imperial College of Science and Technology, Exhibition Road, London SW7 2BX, England.

MATERIALS AND EXPERIMENTAL BEHAVIOUR

The material investigated was structural steel BS4360-50D, supplied in the form of a rolled plate 25mm thick, used in offshore structures. The chemical composition and mechanical properties are given in Table 1.

The butt welded specimens were prepared by manual arc welding of two plates of about 50mm wide, 95mm long and 25mm thick using a C-Mn electrode (3), which is frequently specified for welding of offshore platforms. The joint preparation was a double V. All the welds were ground flat before testing. The chemical and mechanical properties of the weld metal are given in Table 2.

Standard compact type specimens 79.5mm wide, 95.4mm deep and 25mm thick were used in the present study. The notches were orientated perpendicular to the rolling direction and, in the case of butt welded specimens, parallel to the weldment.

The tests were performed in laboratory air and at room temperature (20°C and 50% RH) using three different fatigue machines: a Dowty 60 kN, a Mayes 100 kN, and a Dartec 200 kN.

To investigate the effect of stress ratio and frequency, tests were performed at R -values equal to 0.08 and 0.7, while loading frequencies were 30Hz and 0.25 Hz. All the specimens were tested under identical maximum tensile load (i.e. K_{max}). The minimum load was appropriately adjusted in order to obtain the required stress ratios. A travelling microscope was used to measure the crack length. The crack length measurements on the base metal were made on one side of the specimen since the crack growth was uniform across its thickness. However, with the welded specimens the crack growth was non-uniform across the specimen thickness with one side of the crack leading the other; also, the crack front curvature was sometimes substantial. Thus the crack length measurements were made on both sides of the specimen after each test the specimen was opened up and measured and the crack length corrected for the curvature of the crack front as recommended in ASTM standards (4). The experimental readings of crack length, a , and corresponding numbers of cycles, N , were recorded periodically after suitable crack increments. To calculate the crack growth rate, da/dN , from the experimental data, the secant method was used. The stress intensity factor, K , was calculated using the standard formula recommended for compact-type geometry (5):

$$K = \frac{P}{Bw^{3/2}} \cdot f\left(\frac{a}{w}\right) \quad (1)$$

where $0.3 < a/w < 0.7$. The crack length, a , is the average of the two successive readings used to calculate the corresponding da/dN .

RESULTS

The results of the crack growth rate, da/dN , versus ΔK values for the parent metal and the weldments are shown in Figures 1 to 4 for a range of R -values and loading frequencies. The data correspond with the Paris expression:

$$\frac{da}{dN} = C (\Delta K)^m \quad (2)$$

Figure 1 represents the results obtained in the parent metal tests at 0.25 Hz for R values of 0.08 and 0.07, indicating the effect of stress ratio. Similar, but less pronounced, differences were recorded at 30Hz.

In order to evaluate the effect of frequency on crack growth rate at both R -values, the best fit lines through the results of 0.25 Hz and 30 Hz were plotted and are shown in Figure 2. Similarly, Figure 3 shows the results for the weldments for the identical frequency of 0.25 Hz and the same R -values. Again, a very similar, but stronger, effect of stress ratio and frequency to that of the parent metal may be observed (Figure 4).

Figures 5 to 8 represent a comparison of the results obtained for the parent metal and the weldment under identical testing condition. From these results, we can conclude that for low values of ΔK (below $20 \text{ MN/m}^{3/2}$), the crack growth rate in the weldment is similar to or up to five times slower than in the parent material. At higher frequencies and lower R -values, the crack growth rate in the weldment may be even slower than recorded here.

FRACTOGRAPHY

The weldment fracture surfaces of fatigue cracked specimens (at $R = 0.7$ and 30 Hz) were sectioned and mounted for study in the scanning electron microscope (SEM).

All the variations in the fracture surfaces were examined; it was noted in particular that the dendritic formations might be responsible for the differences in the crack lengths as measured on the sides of the specimen. The formation of dendritic structure has been attributed to the difference in the cooling rate of the weld beads. Figure 9 shows a typical surface close to the specimen side.

The cracks showed a tendency to branching (Figure 10). It can be seen that these branches were random in direction, but there is no evidence that the main crack path was a result of a series of random paths. Also, a high proportion of secondary cracks was often found in a more brittle fracture observed at low ΔK values.

The failure surface showed a number of welding defects which may have some bearing on the results obtained. The most common were 'worm' holes originating from the root of the weldments. The size of these defects varied from a pinhole to a gross defect size (Figure 11). Some defects originated from porosity (figure 12).

The fracture mechanisms observed in the Paris regime were mainly striations, but also microvoid coalescence. A microvoid coalescence area is shown in Figure 13, whereas a typical striated area at $\Delta K = 20 \text{ MN/m}^{3/2}$, $R = 0.7$ and at 30 Hz is presented in Figure 14. A quasi cleavage fracture was observed at very low values of ΔK (7 to $10 \text{ MN/m}^{3/2}$) close to the near threshold region, as shown in Figure 15, and this represents a mixed crack growth in the regime I.

As evidenced by the data (Figure 4) and fractographs (Figure 15), the loading frequency plays an important part in fatigue crack growth. For low frequencies and low ΔK values, cleavage fracture was evident, and this may be connected with the hydrogen embrittlement mechanism. The hydrogen generated may be able to diffuse a certain distance ahead of the crack tip, which results in the crack front advancing at a greater distance per cycle. However for each frequency, there will be a point at which the diffusion of hydrogen within the lattice cannot keep up with the advancing crack and the fracture

mode will change from brittle to a ductile fatigue mechanism. This explains the observed significant increase in the crack growth rate over certain ranges of stress intensity for each frequency associated with the change in fracture mode observed.

DISCUSSIONS

Base Metal

Figures 1 and 2 represent the experimentally determined fatigue crack growth rates, da/dN , as a function of stress intensity factor, ΔK , for a range of stress ratios and frequencies. It can be seen that all data fall approximately on a straight line, confirming that the Paris law for fatigue crack growth is applicable, at least for the investigated region 10^{-6} to 10^{-3} mm/cycle.

Structural materials usually exhibit increasing fatigue crack growth rates with increasing R -values. This is attributed to local static fracture modes at high stress intensity factors (6). In the present investigation, K_{IC2} reached the value $50 \text{ MN/m}^{3/2}$ for $R = 0.08$ and $30 \text{ MN/m}^{3/2}$ for $R = 0.7$ (Figure 2).

Figures 1 and 2 also show that, for the material tested, there was no significant difference in fatigue crack growth rates for the different R -values. In other words, for the load range investigated, the material has sufficient inherent toughness to avoid local static fracture.

Crack closure has often been used to explain the observed effect of stress ratio on fatigue crack growth rates. According to this concept, closure of the crack surfaces may occur at tensile loads during the loading cycle as a result of plastic deformation left in the wake of a growing crack at high stress intensities. This phenomenon reduces the effective stress intensity factor causing crack growth. However, at high stress ratios, the crack remains open for a larger part of the load cycle and thus closure effect becomes less pronounced (1).

It is also possible to explain the effect of stress ratio in terms of environmental effects. Hydrogen in moist air can cause embrittlement at the crack tip, thus leading to increased growth rates. This conclusion is supported by the effect of frequency (Figure 1). At high stress ratios, the crack remains fully open for a larger part of the cycle and, consequently the environmental effects are also maximised. This process was confirmed by the results obtained for the steels tested in vacuum (7) where the influence of stress ratio was minimised.

The Weldment

Figures 3 and 4 present the experimentally determined fatigue crack growth rates, da/dN , as a function of the stress intensity factor, ΔK , in the weldments. Again, these data for welded specimens with the crack growing in the plane of the weld fall approximately on a straight line as observed for the base material.

However, at low ΔK (7 to $15 \text{ MN/m}^{3/2}$), the crack growth rate in the weld metal was lower than the growth rate in the base material (Figures 5 to 8), possibly due to favourable residual stresses.

Residual stresses in butt welded test sections have been investigated in (8). The most significant residual stress component in the weld is the

longitudinal σ_x which can reach the magnitude of yield strength. The transverse stress component, σ_y , is usually substantially smaller. In the present work, no measurement of the residual stress was made, however, a qualitative discussion of the influence of the residual stress follows.

Although stresses parallel to the crack plane and in the transverse direction to the plane of the specimen may not influence the stress intensity factor, they have been shown to influence the plastic flow around the crack (5). A tensile stress component parallel to the crack plane will decrease the plastic flow and a compressive stress component will increase the plastic flow around the crack tip upon loading. Therefore, the net effect over one cycle is not easily predicted. The distribution of longitudinal residual stresses in the direction perpendicular to the crack may induce a closing moment which would resist the opening of the crack and therefore tend to decrease the crack growth rate.

In some tests, especially at low ΔK (7 to $15 \text{ MN/m}^{3/2}$), the crack grew faster on one side of the specimen where the first bead was deposited. On that side, the transverse residual stresses ought to be lower than on the side of the second bead. Also, when grinding the specimen, most of the transverse residual stresses may be released and therefore the crack growth rate ought to be lower.

The influences of R -values is shown in Figures 2 and 4. It can be seen that at low values of ΔK , an increase in R -values from 0.08 to 0.7 has a significant effect on the rate of fatigue crack propagation. The crack closure phenomenon has often been used to account for the observed effect of stress ratio on fatigue crack growth as explained previously. Following this argument it would seem reasonable to say that crack closure can be significant in weldments depending on the magnitude of residual welding stresses which exist in welded joint.

CONCLUSIONS

1. Fatigue crack growth in the parent plate and the weldment of BS 4360 50D steel was investigated. A high stress ratio and a low frequency of loading significantly increased crack growth rates in both parent material and weldment.
2. Fatigue crack growth was faster in the parent material than in the weldment due to the compressive residual stresses in the weldment.

REFERENCES

1. Musuva, J.K., and Radon J.C., 1979, J. Fatigue of Eng. Mats. and Structures 1, 457.
2. Signes, E.G., 1967, British Welding Journal 14, 108.
3. BOC Murex International, August and September 1980.
4. "Tentative Test method for constant load amplitude fatigue crack growth rates above 10^8 m/cycle" ASTM standard E647 - 78T 1978.
5. Wessel, E.T., 1968, Eng. Fract. Mech. 2, 77.

6. Musuva, J.K., and Radon., 1981, "Threshold of Fatigue Crack Growth in Low Alloy Steels", 5th International Conference on Fracture Proceedings "Advances in Fracture Research", Pergamon Press, London, England, 1965.
7. Cooke, R.J., Irving, P.E., Booth, G.S., and Beevers, C.J., 1975, Eng. Fract. Mech. 7, 69.
8. Nordmark, G.E., Muller, L.N. and Kelsey, R.A., 1982, "Effects of Residual Stresses on Fatigue Crack Growth Rates in Weldments of Aluminium Alloy 5456 Plate", ASTM STP 776, 44.

TABLE 1

STEEL BS4360-50D

Chemical Composition (Weight)

Element	C	Si	Mn	P	S	Cr	Mo	Ni	Al	Cu	Nb
%	0.180	0.36	1.40	0.018	0.003	0.11	0.020	0.095	0.035	0.16	0.039

Mechanical Properties

	Direction		
	Longitudinal	Transverse	Through thickness
Yield strength (MN/m ²)	386	382	388
Ultimate tensile strength (MN/m ²)	560	551	563
% elongation (GL equal 3")	30	29	18
% reduction in area	74	68	61

TABLE 2

Welding Electrode BS 639 : E4311 R21 (3)

Chemical Composition (Weight)

Element	C	Mn	Si	S	P
%	0.06	0.58	0.43	0.02 max	0.03 max

Mechanical Properties

Yield strength N/mm ²	448
UTS N/mm ²	510
% Elongation	22
% Reduction of area	50
Charpy V-notch at RT (20°C) 80 joules	

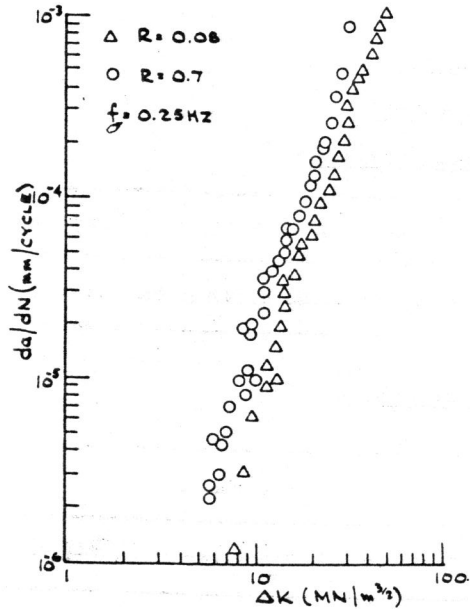


Figure 1 Parent Plate - effect of stress ratio

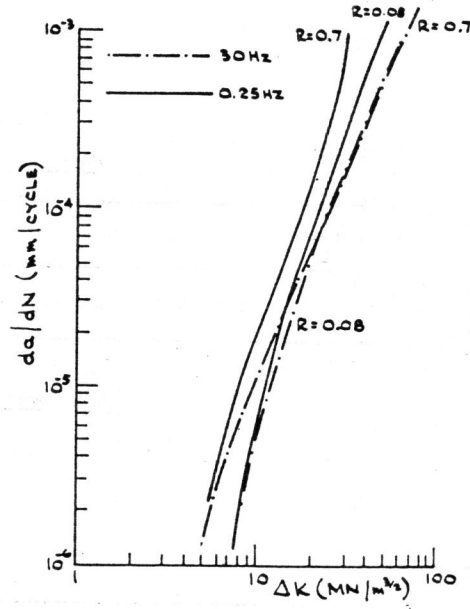


Figure 2 Parent Plate - effect of frequency

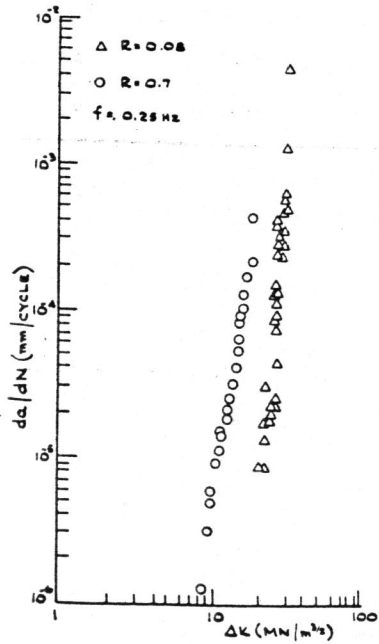


Figure 3 Weldment - effect of stress ratio

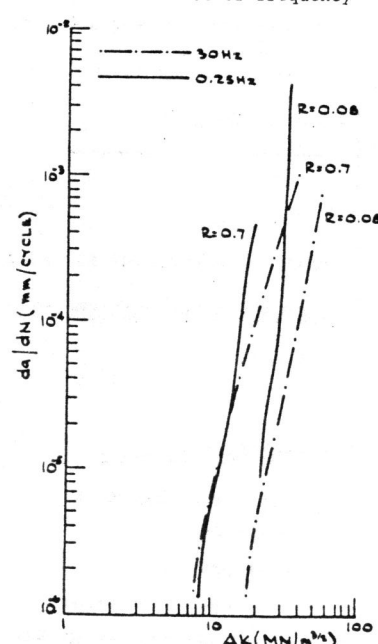


Figure 4 Weldment - effect of frequency

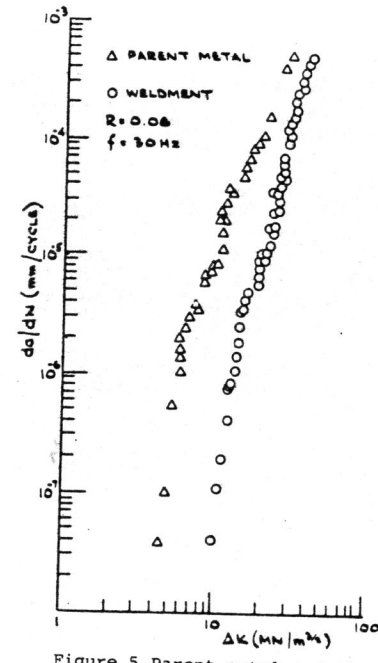


Figure 5 Parent metal and the weldment - R = 0.08, 30 Hz

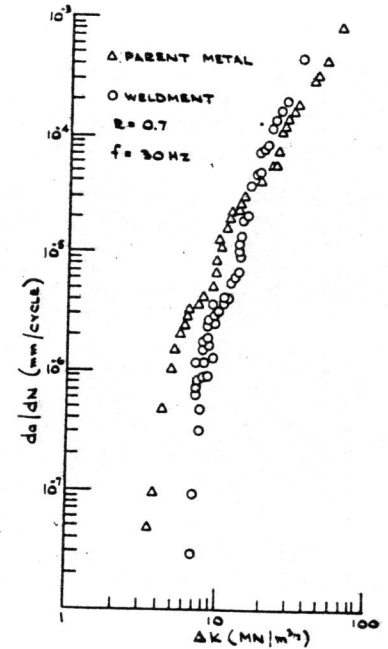


Figure 6 Parent metal and the weldment - R = 0.7, 30 Hz

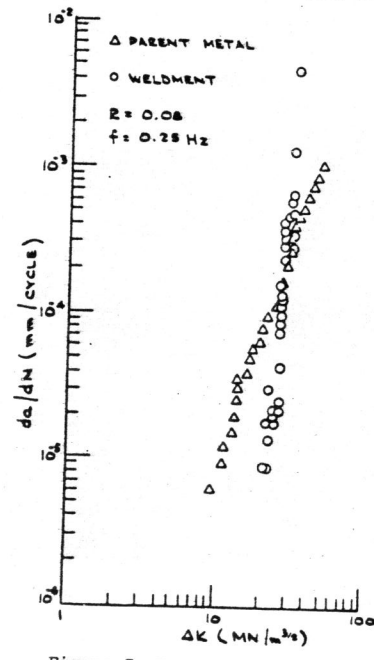


Figure 7 Parent metal and the weldment, - R = 0.08, 0.25 Hz.

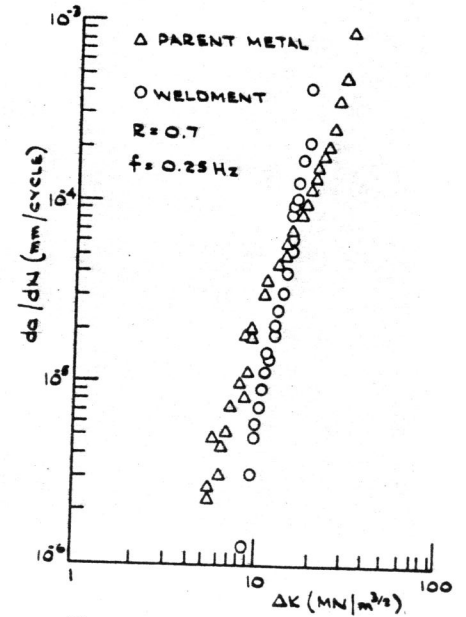


Figure 8 Parent metal and the weldment - R = 0.7, 0.25 Hz.

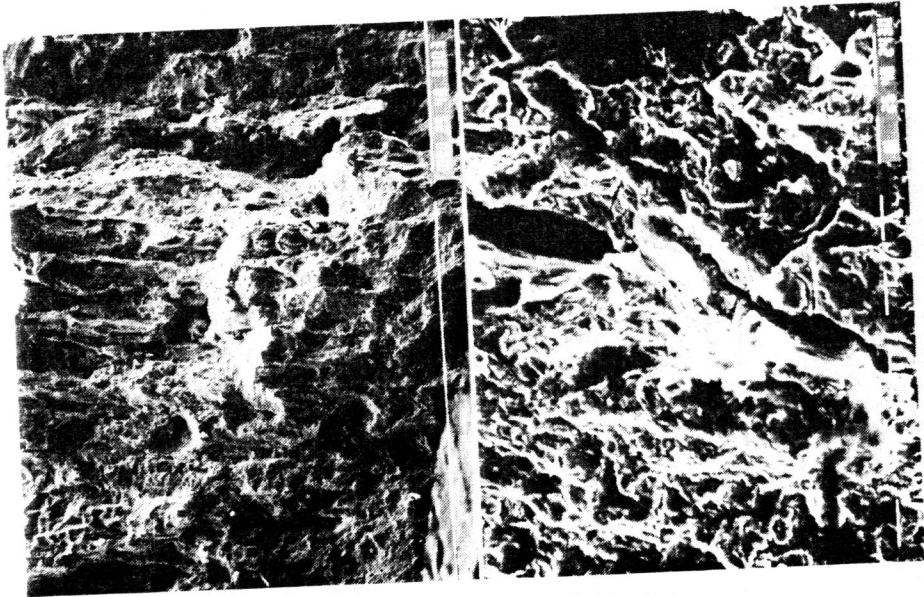


Figure 9 Dendritic formations with columnar grains.

Figure 10 Secondary fatigue cracks

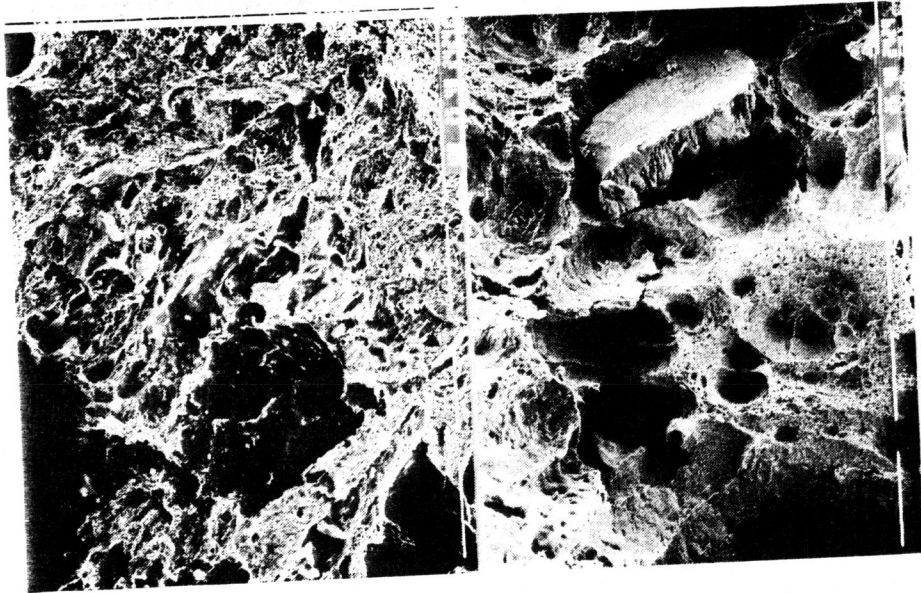


Figure 11 Defects

Figure 12 Porosity

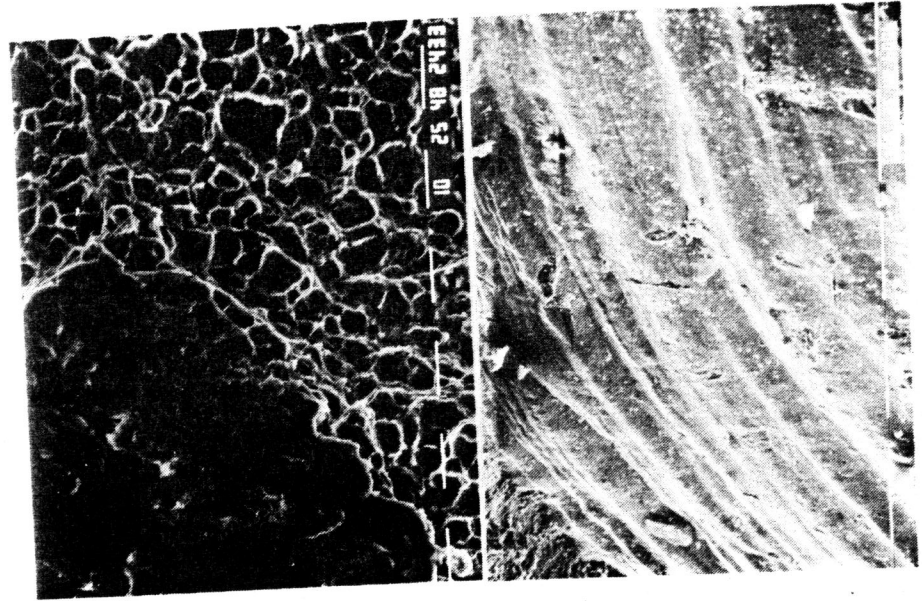


Figure 13 Microvoid coalescence

Figure 14 Fatigue striations

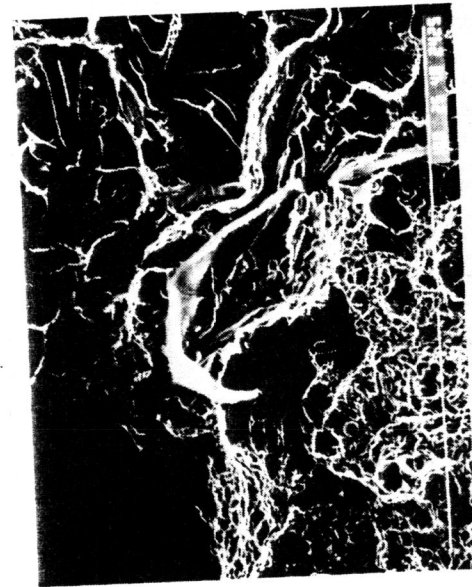


Figure 15 Cleavage